

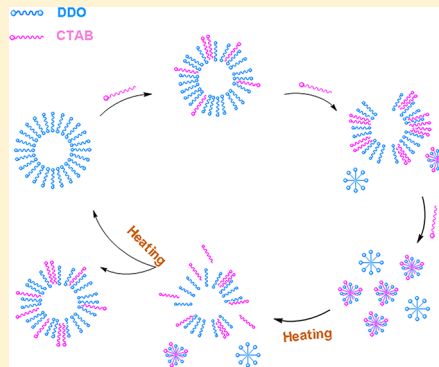
# Realization of the Reversible Vesicle–Micelle Transition of Vitamin-Derived Bolaamphiphiles by Heat Change Monitoring

Yu-Long Sun,<sup>‡</sup> Si-Si Wang,<sup>†</sup> Xue Han,<sup>‡</sup> and Zhong-Xiu Chen<sup>\*,‡</sup>

<sup>‡</sup>Department of Food Quality and Safety, <sup>†</sup>Department of Applied Chemistry, College of Food & Biology Engineering, Zhejiang Gongshang University, Hangzhou, Zhejiang 310035, P. R. China

 Supporting Information

**ABSTRACT:** The real-time energetics involved in the structural change of a zwitterionic vitamin-derived bolaamphiphiles (DDO) vesicles, which were induced by conventional surfactants, such as hexadecyltrimethylammonium bromide (CTAB), sodium dodecyl sulfate (SDS), and Triton X-100 (TX100), was characterized by isothermal titration calorimetry (ITC). Interactions of both CTAB and SDS with DDO were accompanied with considerable heat release whereas the interaction energetics between TX-100 and the vesicles were small. However, the transition of DDO vesicles to micelles did occur upon the addition of all of the three surfactants. Fine inflection points were observed in heat flow enthalpograms, which indicated systematically the change of vesicle structure. By monitoring the interaction of CTAB with DDO, we found that heat release kept constant over a certain concentration range at higher temperatures. The repairing effect of heating was revealed and a reversible transition from micelles to vesicles of DDO was thus realized. Further encapsulation of fluorescein in DDO vesicles proved that the reversible vesicle–micelle transition was controllable. This research demonstrates that ITC combined with complementary analytical methods such as dynamic light scattering (DLS) and transmission electron microscopy (TEM) helps to get the real-time information of the structural changes of vesicles. It also shows that these synthetic novel bolaamphiphiles offer great promise for designing controllable release system.



## INTRODUCTION

Bolaamphiphiles, which consist of two hydrophilic headgroups connected by one or two hydrophobic chains, have drawn increasing attention for their interesting properties since the early 1980s.<sup>1–7</sup> Usually, bolaamphiphiles have superior capability in forming monolayer membranes or vesicles in aqueous solution, which can be widely used as membrane mimetic,<sup>8</sup> drug-delivery systems,<sup>9</sup> microreactors models,<sup>10</sup> and nanoparticle stabilizers.<sup>11</sup> However, many bolaamphiphile-based vesicles can be prepared only in extreme conditions or in the presence of other surfactants.<sup>12,13</sup> Therefore, seeking bolaamphiphiles units that can form vesicles spontaneously without any assistance are attractive in self-assembly research.

The structure of bolaamphiphiles such as the size and planarity of polar group as well as the length of connecting hydrophobic chain strongly affect the spontaneous formation of vesicles. In our previous work, we reported on a designed bolaamphiphile (1,12-diaminododecanediorotate, DDO).<sup>14</sup> The characteristics of the DDO structure are its hydrophilic head groups, which cap the ends of a saturated, C12 linear-hydrocarbon hydrophobe. The end groups with planar structure provide canonical hydrogen-bonding partners for molecular recognition function and make it form vesicle spontaneously. Despite the self-assembly behavior of this bolaamphiphile, a clear picture of the different physical processes leading to the structural changes is still not available.

An ensuing question is whether the assembly and disassociation of the bolaamphiphile vesicles are controllable. To address this question, we investigated the stability and durability of DDO vesicles in the presence of conventional surfactants in this paper. Past studies have shown that solubilization of vesicles to micelles can be realized by the addition of surfactants such as cationic DTAB,<sup>15</sup> anionic SDS,<sup>16</sup> and nonionic Triton X-100<sup>17</sup> or octylglucoside.<sup>18</sup> Bile salt was also reported for the solubilization of phosphatidylcholine vesicles.<sup>19</sup> Moreover, vesicles can get transformed into spherical micelles upon addition of salt<sup>20,21</sup> or by the external forces such as shear.<sup>22</sup> As for micelles to vesicles transition, addition of SDS to cetyltrimethylammonium *p*-toluenesulfonate (CTAPTS) converted the wormlike micelles to vesicles.<sup>23</sup> Introduction of organic additives such as NaNPhS,<sup>24</sup> cholesterol,<sup>25</sup> *n*-octanol,<sup>21</sup> and hexanol<sup>26</sup> could also assist micelles to transform into vesicles. However, the above assembly transition usually takes place irreversibly, i.e., from vesicles to micelles or from micelles to vesicles. Some vesicles formed by more than one component underwent reversible transition at different temperatures.<sup>27</sup> In controllable self-assembly research, designing of reversible micelle-to-vesicle regulations of simple one-component vesicles

Received: July 18, 2012

Revised: September 19, 2012

Published: September 20, 2012

is important for formulations. An early report on a reversible micelle–vesicle transition was about natural dimyristoylphosphatidylcholine (DMPC) vesicles.<sup>15</sup> Another interesting sugar-based gemini surfactant has been reported about the reversible vesicle-to-micelle transition at different pHs.<sup>28</sup> Besides, a novel pH, photoresponsive block copolymer was recently reported to have a reversible morphological transition from micelles to vesicles in the presence of cyclodextrin.<sup>29</sup> To date, the reversible vesicle-to-micelle transition of bolaamphiphiles is rarely reported. We present data demonstrating that the dissociation and re-formation of bolaamphiphile DDO can be easily controlled, which underline the importance of its potential use in drug-delivery systems.

General techniques such as dynamic light scattering (DLS) and transmission electron microscopy (TEM) are often used to characterize the change in structure and size of the assembly. However, these methods only provide averaged information after the aggregation of amphiphiles has accomplished whereby certain important rare events may have been lost. It is urgent to develop convenient methods to get real-time information of the structural changes in the self-assembly process. So far, several techniques have been reported that have the capability to reveal the rotational dynamics of macromolecules in bulk solution, including fluorescence anisotropy, depolarized light scattering, transient electric birefringence, and so forth.<sup>7</sup> Lots of references have evidenced that isothermal titration calorimetry (ITC) is one of the most sensitive techniques to track the energy associated with disassembly processes. The insertion of a surfactant into the bilayer membrane is generally accompanied by a consumption or release of heat, which can be measured fast and reliably with titration calorimeters. Therefore, the characteristic changes in heat flow can be ascribed to interactions between surfactants and vesicles and possible structural changes of the aggregates. Moreover, by adjusting the titration model, we could be able to monitor the enthalpy changes during the dynamic self-assembly process and control the transition between monomers and various aggregates. In the current work, we used ITC to monitor the enthalpy changes associated with assembly process of bolaamphiphiles. DLS and TEM were also used to characterize the change in assembly structure, the size and the dispersion of aggregates. Put together, these three approaches provide a rather detailed picture of the process of solubilization of bolaamphiphiles formed vesicles. Further analysis of the characteristic heat change in vesicle solubilization makes us realize a reversible micelle-to-vesicle transition.

## EXPERIMENTAL SECTION

**Materials.** The surfactants hexadecyltrimethylammonium bromide (CTAB), sodium dodecyl sulfate (SDS), and Triton X-100 (TX100) were purchased from Sigma and were used without further purification. Synthesis of 1,12-diaminododecanediorotate (DDO) was described in detail by previously reported.<sup>14</sup> Ultrapure Millipore (B0500891) water ( $18.2\text{ M}\Omega$ ) was used for the preparation of all solutions.

**Dynamic Light Scattering Measurement (DLS).** Dynamic light scattering (DLS) measurements were performed by a Zetasizer Nano-ZS (Malvern Instruments) with a He–Ne laser (633 nm, 4 mW). The instrument detects the scattered light at an angle of  $173^\circ$ . Sample solutions were filtered through  $0.45\text{ }\mu\text{m}$  Millipore filters before each measurement. All measurements were performed in a temperature-controlled

chamber. Equilibration time was 2 min, and each experiment was repeated three or more times.

**$\zeta$  Potential and Conductivity Measurement.** The  $\zeta$  potentials and conductivity of freshly prepared solutions were determined using the standard capillary electrophoresis cell of Zetasizer Nano ZS from Malvern Instruments at different temperatures without filtering. The equilibration time was 2 min, and each experiment was repeated three or more times.

**Transmission Electron Microscopy (TEM).** A Hitachi 7650 transmission electron microscope operating at a voltage of 120 kV was used for TEM measurements. Phosphortungstic acid (1% (w/v)) was used as the staining agent. A drop of the sample solution ( $10\text{ }\mu\text{L}$ ) was placed onto a carbon Formvar-coated copper grid (200 mesh). Filter paper was employed to absorb the excess liquid. Each experiment was repeated two or more times. The process of adsorption was equilibrated in a thermostatic bath at the needed temperature.

**Isothermal Titration Calorimetry.** An isothermal titration calorimeter (VP-ITC, Microcal Inc., Northampton, MA) was used to measure enthalpies involved in surfactants/bolaamphiphile interactions. Conventional surfactants in the syringe were of 6 mM for CTAB and 1 mM for SDS. In a typical experiment, bolaamphiphile DDO solution (1 mM) was placed in the  $1430\text{ }\mu\text{L}$  sample cell of the calorimeter and surfactant solutions were loaded into the injection syringe. All solutions were prepared in deionized water and were degassed prior to use. The reference cell was filled with deionized water. An initial injection of  $1\text{ }\mu\text{L}$  was made, and then  $10\text{ }\mu\text{L}$  aliquots were injected into the sample cell. The duration of each injection was 20 s, and there was an interval of 360–4500 s between successive injections to achieve complete equilibration. The solution in the titration cell was stirred at a speed of  $307\text{ revolutions min}^{-1}$  throughout the experiment. Control experiments included the titration of conventional surfactants into water, and water into water. Experiments were performed at three different temperatures: 25, 35, and 55 °C. All the results of the ITC experiments were presented in terms of the enthalpy change per injection ( $\Delta H$ ) as a function of surfactant concentration. Each experiment was repeated twice and the reproducibility was within  $\pm 3\%$ .

**Steady-State Fluorescence Spectral Measurements.** Pyrene ( $0.5\text{ }\mu\text{mol L}^{-1}$ ) was dissolved into mixed systems of surfactant and vesicles solution. Fluorescence measurements were performed on a Hitachi F-7000 fluorescence spectrophotometer in aqueous solutions that were degassed before measured. Fluorescence emission spectra of these solutions were recorded employing an excitation wavelength of 335 nm with the exciting and emitting bandwidth of 5.0 and 2.5 nm, and the intensities  $I_1$  and  $I_3$  were measured at the wavelengths corresponding to the first and third vibronic peaks in the fluorescence emission spectrum of pyrene.

## RESULTS AND DISCUSSION

**Monitoring the Energetics of Vesicle–Micelle Transition of DDO in the Presence of Conventional Surfactants by Isothermal Titration Calorimetry.** Isothermal titration calorimetry measurements were carried out at 25 °C with the DDO concentration fixed at 1 mM, which was above its critical aggregation concentration.<sup>14</sup> Cationic surfactant CTAB (6 mM, above its critical micelle concentration, cmc) was initially chosen to induce the disassembly of DDO vesicles. As the surfactant concentration in the injector was above the cmc, the injector contained mainly surfactant micelles. The control experiment was performed by titrating

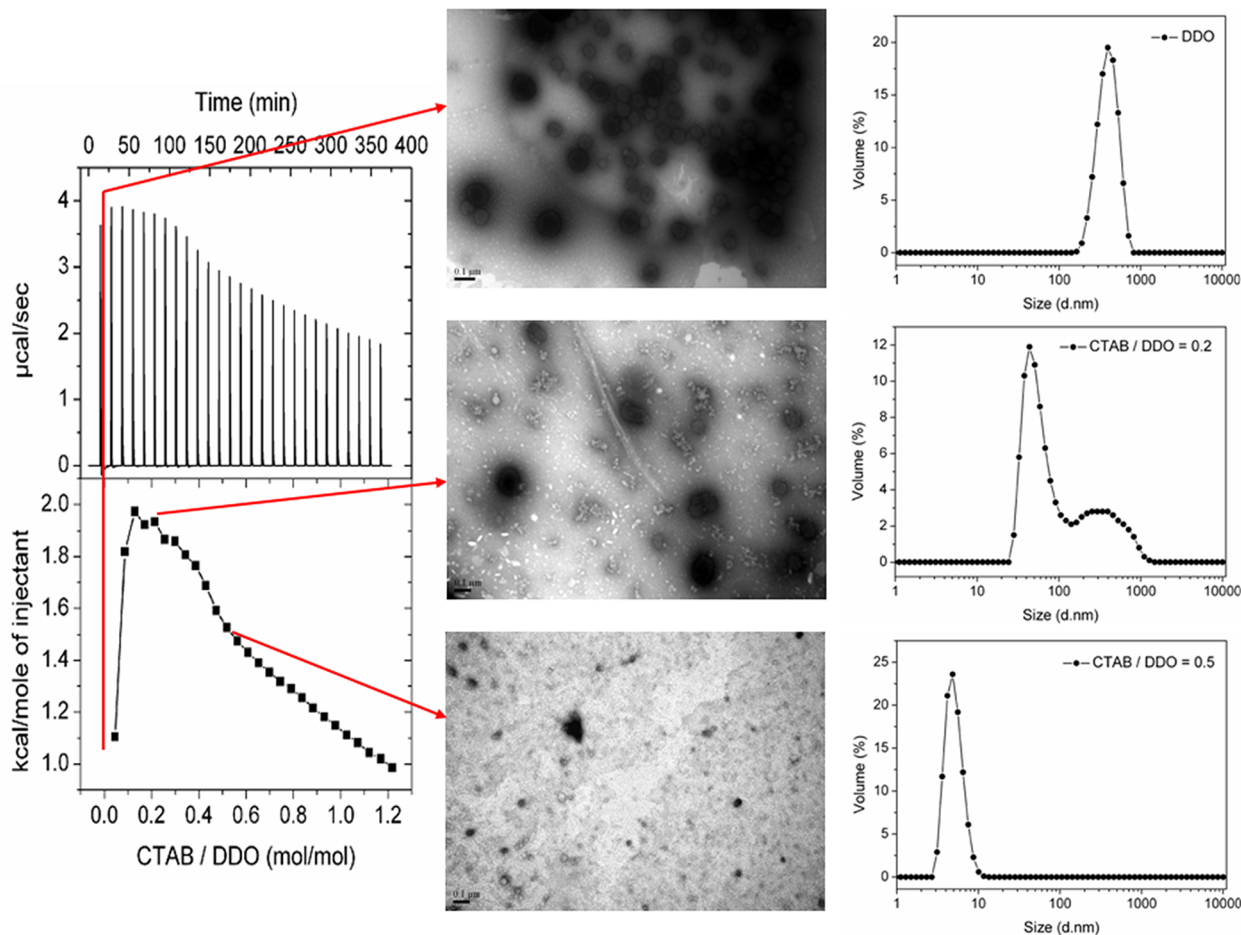


**Figure 1.** Calorimetric curves for the interaction of CTAB with DDO at 25 °C. Structure and size of the CTAB/DDO mixture obtained by TEM and DLS at the overlapping concentration ranges as that in ITC titrations were also shown for comparison.

CTAB micelles into water. Figure 1 is the ITC curve of titrating CTAB micelles into DDO vesicles solution at 25 °C. Endothermic curves were observed in titrating CTAB into both pure water (see further reports) and DDO solution. The enthalpy curve corresponding to the titration of micellized CTAB to DDO vesicles suspension showed an endothermic increase, giving rise to a first endothermic maximum at ratio of  $C_{\text{CTAB}}/C_{\text{DDO}}$  at 0.1/1. The characteristic heat flow can essentially be ascribed to three sequential processes: demicellization of CTAB upon dilution, CTAB-DDO interactions, and surfactant induced structural changes of DDO. The diluted CTAB micelles in the cell may incorporate into the vesicle layers. The partition of the surfactant between water and vesicle layers lasted until the maximum endothermic peak was observed, signaling the DDO vesicles saturated with surfactant monomers. After a certain number of injections, there was an appreciable decrease in peak height due to larger number of vesicles were starting to disassociate. More heat thereby released and counteracted partly by the endothermic energy needed for demicellization of CTAB. This process lasted until the second inflection point appeared after which endothermic heat decreased slightly slowly which indicated the onset of mixed micelles formation. The feature that arises from the analysis of the curves of Figure 1 is the two inflection points in the heat flow. Considering that aggregation of amphiphiles are always accompanied by the energy changes, which make ITC often used to determine the critical aggregation concentration (cac),

we speculate that the inflection points of energy changes in ITC curves characterize the transition between different assemblies of DDO.

To track the detailed dynamic disaggregating of DDO, DLS and TEM were used to follow the change in structure and size of the DDO/surfactant mixture formed at the overlapping concentration ranges as that in ITC titrations. Thus, parallel experiments conducted for the solubilization of DDO vesicles by CTAB can be compared directly. The size distributions of CTAB/DDO mixture at different ratios of  $C_{\text{CTAB}}/C_{\text{DDO}}$  determined by DLS are also shown in Figure 1. Previous report has shown that DDO can form vesicles spontaneously in water at 25 °C.<sup>14</sup> Here only one hydrodynamic diameter distribution at about 396 nm is found which is for individual DDO solutions ( $C_{\text{DDO}} = 1 \text{ mM}$ ) (Figure 1, right) and TEM images had confirmed the existence of vesicles (Figure 1, middle). Two apparent hydrodynamic diameter distributions were observed for CTAB/DDO mixture at  $C_{\text{CTAB}}/C_{\text{DDO}}$  of 0.2/1. Some smaller irregular aggregates were found coexisted with the vesicles in TEM images, implying that solubilization of DDO vesicles took place when CTAB was introduced into the suspension. Meanwhile, ITC curve displayed the first inflection point at almost the same concentration. With more CTAB added into the suspension, the second inflection point was found in ITC curves ( $C_{\text{CTAB}}/C_{\text{DDO}}, 0.5/1$ ). Smaller aggregates with narrower size distribution were observed in DLS peaks. Micelles started to form at this time and then DDO vesicles

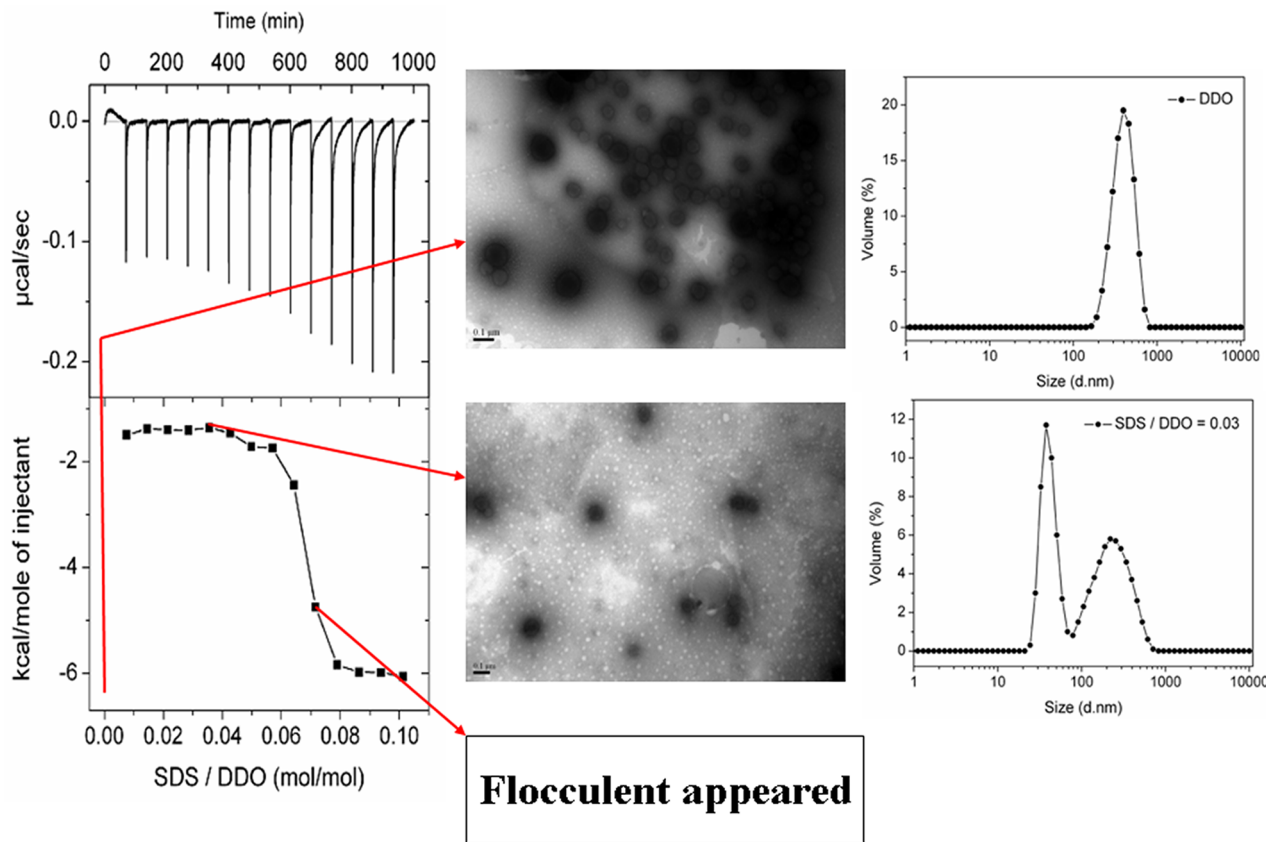


**Figure 2.** Calorimetric curves for the interaction of SDS with DDO at 25 °C. Structure and size of the SDS/DDO mixture obtained by TEM and DLS at the overlapping concentration ranges as that in ITC titrations were also shown for comparison.

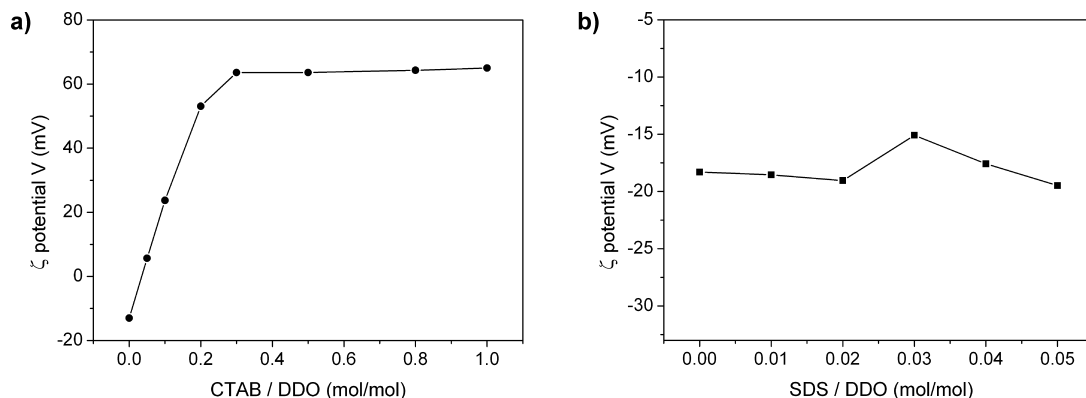


**Figure 3.**  $\zeta$  potential of DDO vesicles ( $C_{DDO} = 1$  mM) upon addition of increased concentration of (a) CTAB and (b) SDS (mol/mol).

could not be found in TEM images, which implied that a considerable number of vesicles had transformed into micelles.

It is noteworthy to say that ITC displayed an endothermic peak when CTAB was added into DDO vesicles. These enthalpy changes were the result of micelle dissociation because the CTAB concentration in the reaction cell was initially below the cmc. As micelle dissociation is thermodynamically favorable below the cmc, the endothermic nature of these peaks indicates that demicellization must lead to an increase in the overall entropy of the system at this temperature. This entropy increase may come from the release of counterions associated with the surfactant head groups and the release of surfactant monomers from micelles when micelles break down to monomers. Our results show that heat release from the interaction of CTAB monomers with DDO vesicles did not

compensate the heat needed to disassemble CTAB micelles, which resulted in an endothermic ITC curve. Disassembling CTAB micelles needs heat input whereas the incorporation of CTAB into vesicles is an exothermic process. This is in line with the results of the transition of mixed vesicles of DEAB/SDS to micelles induced by sodium cholate, which led to an exothermic enthalpies.<sup>30</sup> From the  $\zeta$  potential measurement, we know that DDO bears negative charge in neutral solution. Therefore, binding of CTAB can be considered as the solubilization of the surfactant hydrocarbon chains into the monolayer of DDO. The insertion of CTAB monomers into DDO vesicles was driven by electrostatic force first and then strengthened by hydrophobic interaction. Because CTAB associated with DDO vesicles, a surfactant-rich DDO complex formed and became more charged with surfactant addition.

Repulsive interactions between surfactant headgroups in the vesicle core would expand it, allowing water penetration and the denser packing DDO vesicle loss, thus resulting in the formation of mixed micelles with decreased size.

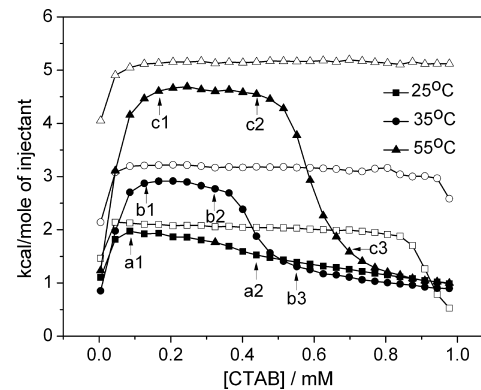
To clarify the effect of the charge of surfactant on the solubilization of DDO vesicles, SDS was also investigated for the interaction with DDO vesicles. ITC displayed an exothermic peaks when SDS was titrated into DDO vesicles. As the surfactant concentration increases, the enthalpy change becomes more exothermic. At a certain surfactant concentration ( $C_{\text{SDS}}/C_{\text{DDO}} = 0.03/1$ ) shown in Figure 2, a sudden increase in the enthalpy was observed, which indicated a strong interaction between SDS and DDO vesicles. Inflection point was also observed on ITC curves just like the case of CTAB/DDO. A similar result was reported by Castro et al.<sup>31</sup> that titration of SDS monomers into water showed a small exothermic process, and the heat release increased in the presence of the diblock copolymer S<sub>15</sub>E<sub>63</sub>. The size distributions of SDS/DDO mixture at different ratios of  $C_{\text{SDS}}/C_{\text{DDO}}$  determined by DLS are shown in Figure 2. With the addition of SDS, DDO vesicles disassembled and the number of vesicles decreased when the ratio of  $C_{\text{SDS}}/C_{\text{DDO}}$  reached 0.03/1. Nevertheless, we found that flocculent occurred when  $C_{\text{SDS}}/C_{\text{DDO}}$  ratios were above 0.07/1 before DDO vesicles were totally destroyed.

Figure 3 is the change of  $\zeta$  potential of DDO in the presence of CTAB or SDS. Increased CTAB made DDO vesicles bear more and more negative charges, which resulted in a stable colloid solution. Unlike CTAB, addition of SDS led to the decrease of charge on the vesicle (less than 30 mV), which could account for precipitation. It is reasonable to suppose that precipitation will take place if two surfactants bearing opposite charge meet. In this case, as both SDS and DDO bear negative charge, thus the hydrophobic interaction is considered the primary driving force for the observed binding due to the better-matched hydrogen carbon chains of the two surfactants. It is well established that cationic surfactants interact less strongly with nonionic polymers than anionic surfactants. This difference has been ascribed to steric hindrance due to the voluminous trimethylammonium headgroup.<sup>32</sup> In this case, small surfactant aggregates around the vesicles may form cooperatively just like the interaction of SDS with the polymers.<sup>33</sup> The interaction of SDS and CTAB with DDO are both  $\Delta H$  and  $\Delta S$  favorable, where the negative  $\Delta H$  indicates the hydrophobic interaction and the entropy gain is attributed to the disruption of water structure upon the formation of surfactant micelles on DDO vesicles.

In contrast to SDS and CTAB, the titration curve for TX100 in DDO was close to that in water, suggesting that interaction energetics between this surfactant and the vesicles were small (see Supporting Information). However, the solubilization of DDO vesicles did take place upon the addition of TX100. Two hydrodynamic diameter distributions were clearly observed for TX100/DDO mixture at  $C_{\text{TX100}}/C_{\text{DDO}} = 0.05/1$ . With more TX100, the micelle peak played a leading role in the size distribution, which indicated that considerable number of vesicles had transformed into micelles. Finally, after  $C_{\text{TX100}}/C_{\text{DDO}}$  reached 0.4/1, only a micelle peak at about 7 nm existed in the DLS plot, which suggested that nearly all of DDO vesicles had turned into micelles, TEM experiments supported the disappearance of DDO vesicles. TX100 is often used to destroy the membrane of cell. The mechanism involved the hydrogen bond formation between the polar polyethylene

group of TX100 and phospholipid bilayer of the cell, which results in a change of the interface tension and solubilization of the cell membrane.<sup>17</sup> DDO is a zwitterionic surfactant that forms a vesicle with recognition group on its surface,<sup>14</sup> hydrogen bond formation may account for the easy solubilization of the vesicle.

**Calorimetric Investigation of Temperature Effect on the Solubilization of DDO Vesicles by CTAB.** The above results showed that the aggregation information of the dynamic disassembly of DDO vesicles in the presence of SDS and CTAB were involved in ITC curves. To get a better understanding of the energetics of solubilization of DDO vesicles, we extended the ambient titration to higher temperatures and addressed special attention to the structural evolution of DDO induced by CTAB. The ITC results obtained from the interaction between CTAB and DDO vesicles at three temperatures were summarized in Figure 4. A series of relatively larger



**Figure 4.** Calorimetric curves for the dilution of 6 mM CTAB in 1 mM DDO solution at 25 °C (■), 35 °C (●), and 55 °C (▲). The corresponding open symbols represent the dilution of 6 mM CTAB in water at each temperature.

endothermic peaks were observed when the surfactant solutions were injected into the reaction cell. Disassociating CTAB micelles became more endothermic as the temperature increased. This was also observed for other cationic surfactants such as DTAB.<sup>33</sup> The cmc of the CTAB, which can be determined from the inflection point in the  $\Delta H$  versus surfactant concentration curves, increased with the elevated temperature. The decreased cmc in CTAB was consistent with the destabilization of micelles due to an increase of electrostatic repulsion between CTAB head groups in the covered temperature range. The curves representing the change in the observed enthalpies with CTAB concentration for dilution of CTAB into pure water were higher (more endothermic) than those for dilution of CTAB in DDO vesicles solutions within the present concentration range. A different behavior was observed for the interaction of SDS with poly(ethylene oxide) (PEO), where titration of SDS into polymer solutions displayed a higher heat uptake than those for dilution of SDS in pure water.<sup>34</sup> The enthalpy values for the dilution of cationic CTAB in the presence of DDO were also not in line with that of polymer, in which the mixed enthalpies were more positive than the dilution enthalpies.<sup>33</sup>

Although ITC curves go in a similar way at higher temperatures, these profiles change notably. At 25 °C, three parts of the isotherms can be assigned clearly according to “three-stage” model of surfactant-induced vesicle solubiliza-

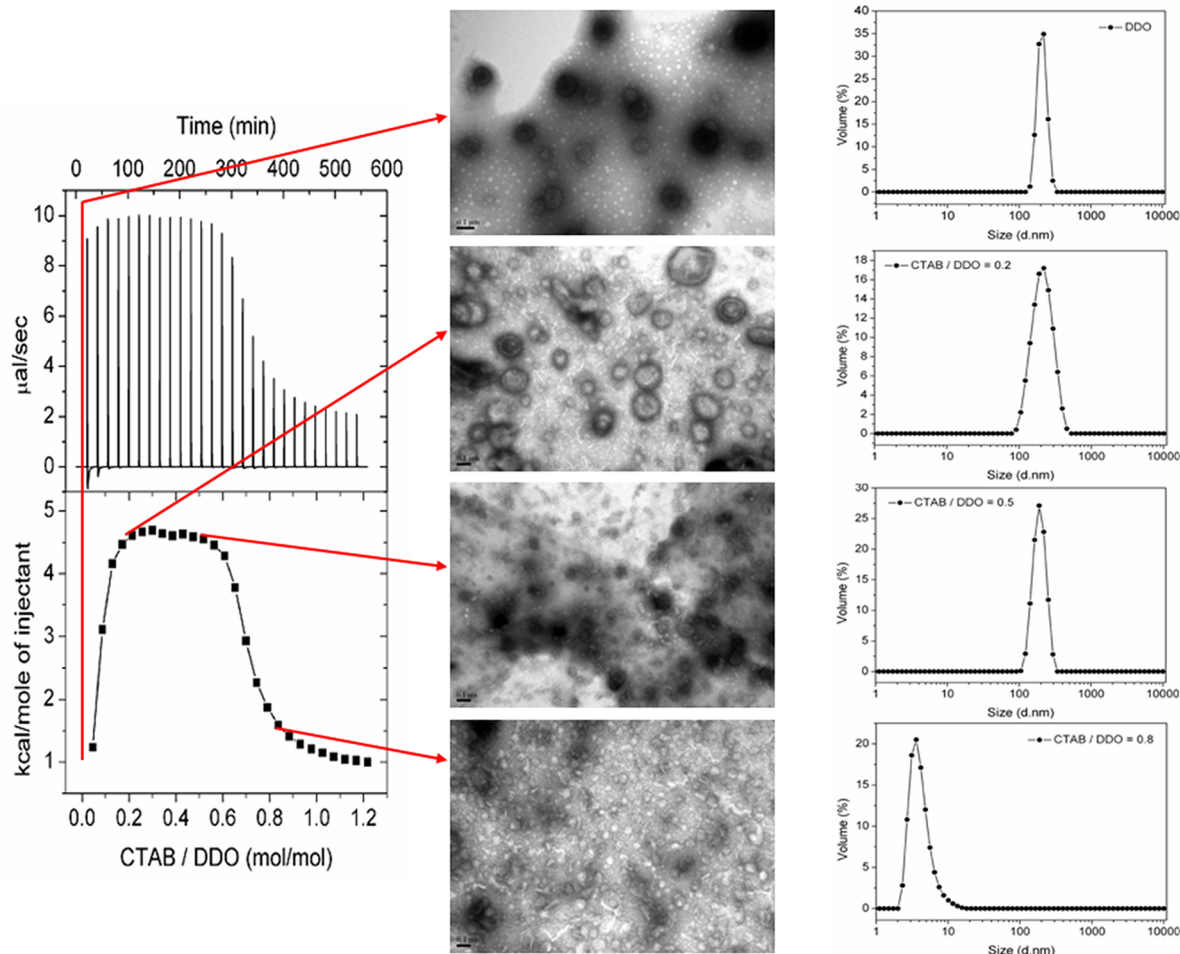


**Figure 5.** Calorimetric curves and structure and size of the CTAB/DDO mixture obtained by TEM and DLS at the overlapping concentration ranges for the interaction of CTAB with DDO at 55 °C.

tion.<sup>35</sup> Detailed examination revealed that the vesicles were broken when  $C_{\text{CTAB}}/C_{\text{DDO}}$  is above 0.1/1(a1) in ITC curves, followed by a coexistence range with vesicles and micelles from a1 to a2 and then all the vesicles transformed into micelles occurred from the second inflection point (a2,  $C_{\text{CTAB}}/C_{\text{DDO}} = 0.5/1$ ). At 35 and 55 °C, three inflection points (b1, b2 and b3; c1, c2 and c3) were observed, respectively, but visible solubilization of vesicles was found to start at b2 and c2. Vesicles and micelles coexisted until b3 and c3 occurred after which only pure micelles survived in the solution. As mentioned above, the first endothermic peak at 25 °C was supposed to signal the onset of the solubilization process. However, the solubilizations were delayed at higher temperatures implying a reduced partitioning of CTAB into DDO layers. Figure 5 showed the structure and the size of DDO vesicles at 55 °C upon addition of CTAB at exactly the same ratio where the inflection point occurred in ITC plots. It is noteworthy to mention that we caught the enlarged DDO images, which could witness some transient aggregates when the DDO vesicles were inserted by CTAB monomers. At the second inflection point of ITC curve where the ratio of CTAB and DDO was 0.5/1, the number of DDO vesicles started to decrease because lots of vesicles had been saturated by CTAB and could not hold for stable vesicles. When  $C_{\text{CTAB}}/C_{\text{DDO}}$  ratios were above 0.8/1, nearly all of DDO vesicles turned into micelles and only a peak at about 6 nm on DLS was observed. TEM also confirmed the disappearance of DDO vesicles. These

results supported that the aggregates transition took place exactly at the ratio of CTAB and DDO where the inflection point occurred in ITC plots. On the other hand, increased temperature made DDO get more time to survive before being destroyed by CTAB.

Another feature was that a plateau of enthalpy was found at 35 and 55 °C. Detailed examination of Figure 4 revealed that the endothermic heat did not decrease immediately at 35 °C when the concentration of CTAB was above  $b_1$ . Instead, constant enthalpy was observed until the concentration of CTAB reached 0.25 mM ( $b_2$  in Figure 4). A prolonged energy plateau was found at 55 °C. The solubilization of DDO vesicles by CTAB in the ITC cell consisted of consecutive steps such as demicellization of the CTAB followed by the interaction of CTAB with DDO and the broken of the DDO vesicles. As DDO tended to form vesicles at high temperatures (with cac decreased) and CTAB showed opposite behavior (with cmc increased which was shown in the control in Figure 1), it was reasonable for CTAB to uptake more heat to solubilize DDO vesicles at an elevated temperature. It can be seen that the shape of the curves did not change from 35 to 55 °C, but more heat was needed when the temperature increased. This indicated that solubilization was less favorable at higher temperatures, which resulted in more surfactants required for the saturation of DDO vesicles and more heat adsorption. The increasing temperature led to a progressive longer plateaus region of enthalpy and the delay of CTAB concentration at

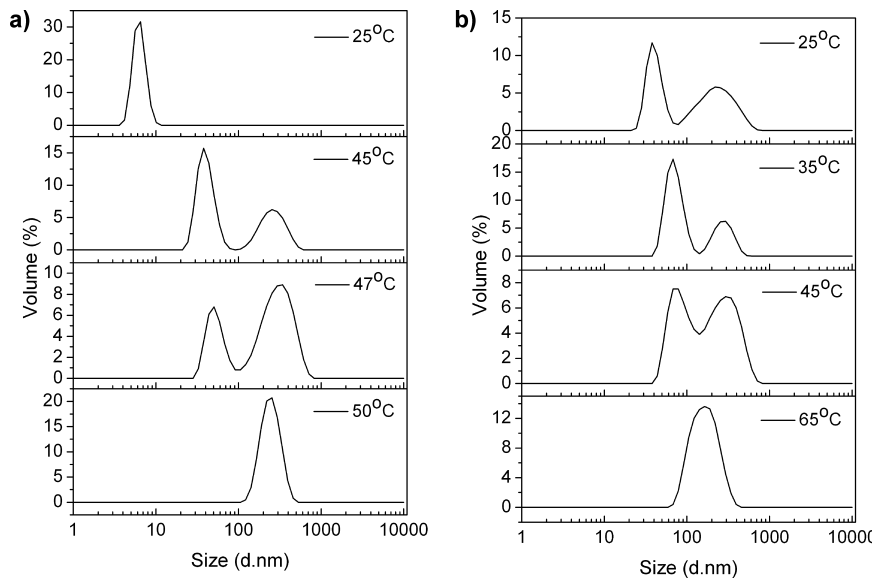


**Figure 6.** Change of hydrodynamic diameter distribution of the mixed micelles solution upon heating: (a)  $C_{CTAB}/C_{DDO} = 0.5/1$ (mol/mol); (b)  $C_{SDS}/C_{DDO} = 0.03/1$ (mol/mol).  $C_{DDO} = 1$  mM.

which all the vesicles disassembled into micelles. These results suggested that the tendency of CTAB molecules to interact with DDO decreased with temperature. The horizontal heat plateau between the two inflection points meant that the reaction heat kept constant with further addition of CTAB over a certain concentration range. A similar “isenthalpic” process was observed in BSA bound to the PAH.<sup>36</sup> From the results of the control titration of CTAB into water, we can see that demicellization of the CTAB was endothermic. It is also known that interaction of surfactant monomers or micelles with liposome is an exothermic process<sup>15</sup> whereas the incorporation of EO groups into SDS micelles is an endothermic process, due to significant dehydration of PEO.<sup>34</sup> In the current report, the overall change in enthalpy due to CTAB-DDO interaction can be estimated by subtracting the integral heats of dilution of CTAB in vesicle solution from those in water. Hence, the incorporation of CTAB into DDO vesicles was expected to be an exothermic process. However, the total observed enthalpy was positive and only monomeric CTAB existed in the cell after the first inflection point occurred. This, together with the fact that more heat was needed at the higher temperature proves that something endothermic happens that may account for the heat plateau in ITC titration. Previous results showed that DDO vesicle formation was an uptake of heat.<sup>14</sup> Therefore, we speculated that vesicles formed coinstantaneously when the temperature increased. Heating may offer a repairing effect, which helps the broken vesicle re-form the new ones.

**Realization of a Reversible Vesicle–Micelle Transition of DDO Vesicles by Heating.** To test our hypothesis that heat input is helpful for the formation of the vesicles of DDO, the broken DDO vesicles that were solubilized by CTAB at ambient temperature were subjected to heating. Figure 6 was the size distribution of the mixed system ( $C_{CTAB}/C_{DDO} = 0.5/1$ ) as a function of temperature determined by DLS. When the temperature was below 40 °C, only mixed micelles with an average hydrodynamic diameter of 7 nm were present. However, the situation was different when the temperature increased to 45 °C. DLS data changed from monomodal to bimodal distributions, and the hydrodynamic diameter of the CTAB/DDO mixed micelles disappeared and two new peaks

were found. One was at 38 nm, which may come from elongated micelles, and another was at 255 nm, which was presumably the hydrodynamic diameter of vesicles. This transition from micelles to vesicles continued as the temperature increased. At 47 °C, the peak corresponding to the elongated micelles shrunk compared with that of 45 °C whereas the vesicles peak increased, suggesting more and more vesicles formed. At temperatures above 50 °C, the peak assigned to elongated micelles disappeared in the DLS plot, leaving the peak of vesicles. Moreover, the peak at about 5 nm that existed only for the micelle was replaced by the peak at about 190 nm that accounted for vesicles when the temperature increased from 25 to 55 °C. TEM images also showed vesicles re-formed after heating the micelle solution. The dimensions and the shape of the newly formed vesicles were similar to that of former DDO vesicles.

As for SDS/DDO systems, we also observed the micelle to vesicle transition upon heating from DLS plot (data not shown). In line with our results, Majhi et al. claimed a temperature-induced micelle-vesicle transition in lipid-surfactant mixed systems.<sup>15</sup> Yin et al. reported a temperature-controlled vesicle aggregation in a catanionic surfactant system of sodium *n*-dodecyl sulfate (SDS)/*n*-dodecyltributylammonium bromide (DTBAB).<sup>37</sup> But it was also reported that heating could also induce vesicles to transform to micelles. For example, cetyltrimethylammonium 3-hydroxynaphthalene-2-carboxylate (CTAHNC) could transform to long wormlike micelles at temperatures higher than about 50 °C.<sup>38</sup> The vesicles formed by CTAB and 5-methyl salicylic acid (5mS) could transform into long, flexible wormlike micelles by heating the solution beyond a critical temperature.<sup>27</sup> In our results, the repaired vesicles would return to mixed micelles if they were cooled, which suggested the characteristic repairing effect of heating.

**Controllable Release of Fluorescein Encapsulated in DDO Vesicles.** To investigate the possible use of reversible aggregation of DDO vesicles for controllable release, pyrene used as fluorescence probe was encapsulated in the vesicles. The ratio of the intensity of the first and the third vibronic peak in the fluorescence spectra of pyrene ( $I_1/I_3$ ) is very sensitive to

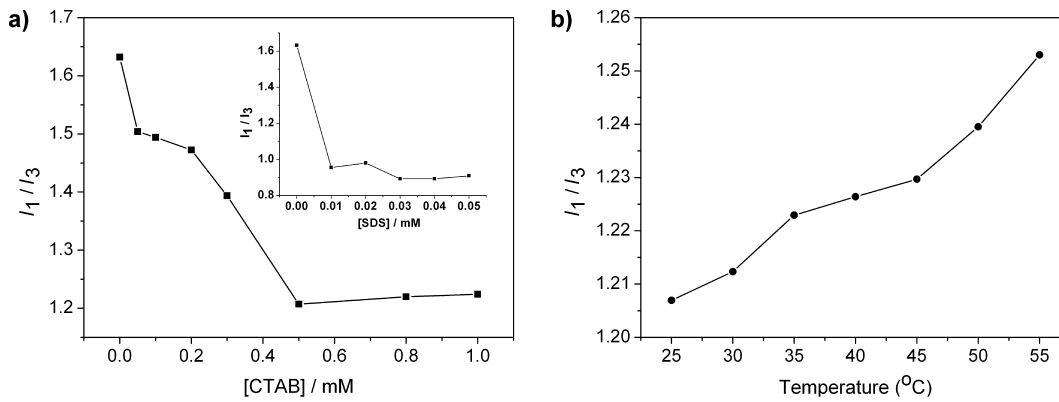


**Figure 7.** Change of  $I_1/I_3$  band ratio in the fluorescence spectra of pyrene (a) dissolved in 1 mM DDO solution with varying concentration of CTAB or SDS at 25 °C and (b) in mixed system of CTAB/DDO (0.5/1) as a function of temperature.

solvent polarity and therefore has been widely used as a measure of the micropolarity of membrane.<sup>39</sup> Pyrene, which was solubilized in the interiors of the micelles, was used as the indicator for the micropolarity change when vesicles endured structural transition. Figure 7a shows the change of  $I_1/I_3$  with surfactant at varying concentrations added to a constant DDO concentration of 1 mM. The higher value of  $I_1/I_3$  indicated a more polar environment. A decrease of the  $I_1/I_3$  ratio was observed when an increased concentration of CTAB was introduced into the DDO vesicles solution. The results implied that pyrene initially solubilized in DDO vesicles layers was released and then entered the more ordered layers of the mixed micelles or the interior of the vesicles. In the initial stage of the solubilization, the insertion of surfactant into the vesicle led to more dense layers with less polarity due to the strengthened hydrophobic interaction. On the other hand, large vesicles turned into small micelles would provide more nonpolar membrane area. Both results contributed to the decrease of  $I_1/I_3$ . The minimum value  $I_1/I_3$  ratio was obtained when DDO vesicles totally turned into micelles or coexisted vesicles and micelles. It was also found that less SDS led to a considerable decrease of  $I_1/I_3$ , which implied the stronger interaction between SDS and DDO. The matched length (both have 12 CH<sub>2</sub> connected group) between the two surfactants makes SDS accommodate well in the monolayer of DDO vesicle, leaving its negative headgroup close to positive ammonium group of DDO. The stronger hydrophobic interaction between the hydrocarbon chains at the same length led to the lower value of  $I_1/I_3$ , whereas the electrostatic attraction between the charged group may be the reason for precipitate formation. Figure 7b showed that, upon heating, the value of  $I_1/I_3$  increased slightly, indicating that the fluorescein was reversibly encapsulated into the vesicles. Because the value of  $I_1/I_3$  of pyrene decreased with the elevated temperature in water,<sup>39</sup> this might offset some of the increased intensity of fluorescence and thus lead to insignificant change of the value of  $I_1/I_3$ .

Figure 8 is a schematic illustrating the reversible vesicle–micelle transition of DDO vesicles. The conventional surfactants such as CTAB and SDS can induce the solubilization of the vesicles, which make the vesicles enlarge initially followed by breaking up to micelles. To realize the reversible micelle–vesicle transition, heating is an effective way to guide the broken vesicles to close. It is noteworthy that dimyristoylphosphatidylcholine (DMPC) vesicles have been solubilized by SDS or dodecyltrimethylammonium bromide (DTAB) and the formed micelles can also converted into

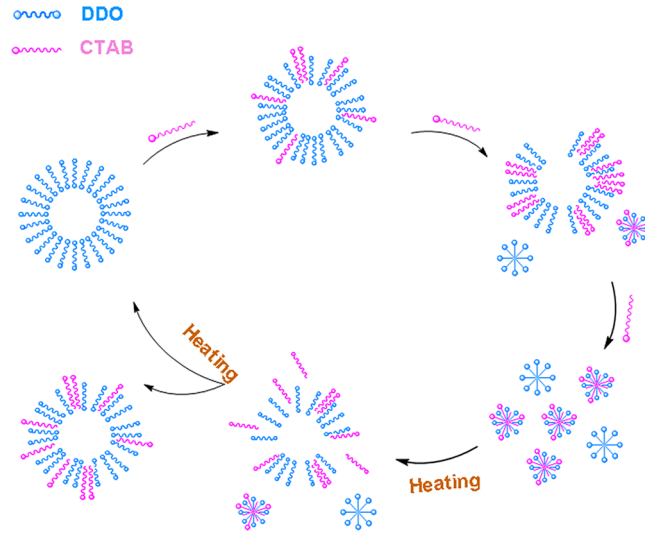


**Figure 8.** Schematic illustration of the reversible vesicle–micelle transition of DDO vesicles.

vesicles by heating.<sup>15</sup> Compared with the natural phosphatidylcholine vesicle, the synthetic DDO vesicle based on vitamin-derived bolaamphiphiles makes its structure adjustable. It has superiority both for encapsulation and for molecular recognition due to its modified headgroup on the vesicle surface.<sup>40</sup>

## CONCLUSIONS

In summary, a variety of complementary analytical methods were used to characterize the interactions between conventional surfactants and vesicles formed from a novel bolaamphiphiles. Interaction of CTAB and SDS with DDO was found exothermic whereas that for TX100 with DDO was small. However, the solubilization of DDO vesicles did occur upon the addition of all of the three surfactants. Noteworthy to say that the heat flow in ITC enthalpograms contain lots of information involved in the interaction in which the inflection points always indicate the change of the vesicle assembly. By monitoring the heat of the interaction of CTAB with DDO at different temperatures, we found a constant enthalpy over a certain concentration range of CTAB during the disassembly of the vesicles. Detailed analysis of the energetics in the vesicle solubilization makes us realize a reversible micelle to vesicle transition. Further encapsulation of pyrene in DDO vesicles proved that the vesicle–micelle transition was reversible which

made the fluorescein release controllable. The current research demonstrates that these novel bolaamphiphiles have a promising potential in model cell mimetic and drug-delivery systems. The isothermal titration calorimetry technique combined with DLS and TEM could provide real-time information of the structural changes of DDO, which makes it possible for recording the thermodynamic fingerprint and guiding the controllable self-assembly of the vesicles.

## ■ ASSOCIATED CONTENT

### Supporting Information

Results of the titration of TX-100 to DDO vesicles solution (cac determined by ITC) along with the specific conductivity versus DDO concentration at different temperature. This material is available free of charge via the Internet at <http://pubs.acs.org>.

## ■ AUTHOR INFORMATION

### Corresponding Author

\*E-mail: zhxchen@ustc.edu.

### Notes

The authors declare no competing financial interest.

## ■ ACKNOWLEDGMENTS

The authors are grateful to the National Nature Science Foundation of China for financial support (NSFC, No. 20973155).

## ■ REFERENCES

- (1) Fuhrhop, J. H.; Fritsch, D. *Acc. Chem. Res.* **1986**, *19*, 130–137.
- (2) Escamilla, G. H.; Newkome, G. R. *Angew. Chem., Int. Ed. Engl.* **1994**, *33*, 1937–1940.
- (3) Fuhrhop, J. H.; Wang, T. Y. *Chem. Rev.* **2004**, *104*, 2901–2937.
- (4) Sun, X. L.; Biswas, N.; Kai, T.; Dai, Z. F.; Dluhy, R. A.; Chaikof, E. L. *Langmuir* **2006**, *22*, 1201–1208.
- (5) Yan, Y.; Lu, T.; Huang, J. B. *J. Colloid Interface Sci.* **2009**, *337*, 1–10.
- (6) Chen, Y. X.; Liu, Y.; Guo, R. *J. Colloid Interface Sci.* **2009**, *336*, 766–772.
- (7) Chen, Y. X.; Liu, Y.; Guo, R.; Xian, S. Y. *J. Solution Chem.* **2011**, *40*, 48–60.
- (8) Li, Q. X.; Mittal, R.; Huang, L. J.; Travis, B.; Sanders, C. R. *Biochemistry* **2009**, *48*, 11606–11608.
- (9) Brunelle, M.; Polidri, A.; Denoyelle, S.; Fabiano, A. S.; Vuillaume, P. Y.; Laurent-Lewandowski, S.; Pucci, B. *C. R. Chim.* **2009**, *12*, 188–208.
- (10) Song, B.; Wu, G. L.; Wang, Z. Q.; Zhang, X.; Smet, M.; Dehaen, W. *Langmuir* **2009**, *25*, 13306–13310.
- (11) Sistach, S.; Rahme, K.; Pérignon, N.; Marty, J. D.; Viguerie, N. L.; Gaufré, F.; Mingotaud, C. *Chem. Mater.* **2008**, *20*, 1221–1223.
- (12) Yan, Y.; Xiong, W.; Huang, J. B.; Li, Z. C.; Li, X. S.; Li, N. N.; Fu, H. L. *J. Phys. Chem. B* **2005**, *109*, 357–364.
- (13) Visscher, I.; Engberts, J. B. F. N. *Langmuir* **2000**, *16*, 52–58.
- (14) Chen, Z. X.; Su, X. X.; Deng, S. P. *J. Phys. Chem. B* **2011**, *115*, 1798–1806.
- (15) Majhi, P. R.; Blume, A. *J. Phys. Chem. B* **2002**, *106*, 10753–10763.
- (16) Yan, Y.; Hoffmann, H.; Drechsler, M.; Talmon, Y.; Makarsky, E. *J. Phys. Chem. B* **2006**, *110*, 5621–5626.
- (17) López, O.; de la Maza, A.; Coderch, L.; López -Iglesias, C.; Wehrli, E.; Parra, J. L. *FEBS Lett.* **1998**, *426*, 314–318.
- (18) Walter, A.; Kuehl, G.; Barnes, K.; VanderWaerdt, G. *Biochim. Biophys. Acta* **2000**, *1508*, 20–33.
- (19) Hildebrand, A.; Neubert, R.; Garidel, P.; Blume, A. *Langmuir* **2002**, *18*, 2836–2847.
- (20) Mohanty, A.; Patra, T.; Dey, J. *J. Phys. Chem. B* **2007**, *111*, 7155–7159.
- (21) Lu, T.; Han, F.; Li, Z. C.; Huang, J. B.; Fu, H. L. *Langmuir* **2006**, *22*, 2045–2049.
- (22) Mendes, E.; Oda, R.; Manohar, C.; Narayanan, J. *J. Phys. Chem. B* **1998**, *102*, 338–343.
- (23) Kaler, E. W.; Herrington, K. L.; Murthy, A. K.; Zasadzinski, J. A. *N. J. Phys. Chem.* **1992**, *96*, 6698–6707.
- (24) Kawasaki, H.; Imahayashi, R.; Tanaka, S.; Almgren, M.; Karlsson, G.; Maeda, H. *J. Phys. Chem. B* **2003**, *107*, 8661–8668.
- (25) Cano-Sarabia, M.; Angelova, A.; Ventosa, N.; Lesieur, S.; Veciana, J. *J. Colloid Interface Sci.* **2010**, *350*, 10–15.
- (26) Oda, R.; Bourdieu, L.; Schmutz, M. *J. Phys. Chem. B* **1997**, *101*, 5913–5916.
- (27) Davies, T. S.; Ketner, A. M.; Raghavan, S. R. *J. Am. Chem. Soc.* **2006**, *128*, 6669–6675.
- (28) Johnsson, M.; Wagenaar, A.; Engberts, J. B. F. N. *J. Am. Chem. Soc.* **2003**, *125*, 757–760.
- (29) Jin, Q.; Luy, C.; Ji, J.; Agarwal, S. *J. Polym. Sci., Part A: Polym. Sci.* **2012**, *50*, 451–457.
- (30) Jiang, L. X.; Wang, K.; Deng, M. L.; Wang, Y. L.; Huang, J. B. *Langmuir* **2008**, *24*, 4600–4606.
- (31) Castro, E.; Taboada, P.; Barbosa, S.; Mosquera, V. *Biomacromolecules* **2005**, *6*, 1438–1447.
- (32) Anthony, O.; Zana, R. *Langmuir* **1994**, *10*, 4048–4052.
- (33) Loh, W.; Teixeira, L. A. C.; Lee, L. T. *J. Phys. Chem. B* **2004**, *108*, 3196–3201.
- (34) da Silva, R. C.; Loh, W.; Olofsson, G. *Thermochim. Acta* **2004**, *417*, 295–300.
- (35) Lichtenberg, D. *Biochim. Biophys. Acta* **1985**, *821*, 470–478.
- (36) Ball, V.; Winterhalter, M.; Schwinte, P.; Lavalle, P.; Voegel, J. C.; Schaaf, P. *J. Phys. Chem. B* **2002**, *106*, 2357–2364.
- (37) Yin, H. Q.; Huang, J. B.; Gao, Y. Q.; Fu, H. L. *Langmuir* **2005**, *21*, 2656–2659.
- (38) Hassan, P. A.; Valaulikar, B. S.; Manohar, C.; Kern, F.; Bourdieu, L.; Candau, S. *J. Langmuir* **1996**, *12*, 4350–4357.
- (39) Nivaggioli, T.; Alexandridis, P.; Hatton, T. A. *Langmuir* **1995**, *11*, 730–737.
- (40) Chen, Z. X.; Cao, C.; Deng, S. P. *Acta Phys. Sin.* **2012**, *28*, 1320–1328.